
HorizonDrive: Self-Corrective Autoregressive World Model for Long-horizon Driving Simulation

Conglang Zhang^{1*} Yifan Zhan^{2*} Qingjie Wang³ Zhanpeng Ouyang³ Yu Li⁴
 Zihao Yang⁵ Xiaoyang Guo⁶ Weiqiang Ren³ Qian Zhang³ Zhen Dong¹
 Yinqiang Zheng² Wei Yin^{3‡} Zhengqing Chen^{3†}

¹Wuhan University ²The University of Tokyo ³Horizon Robotics ⁴Tsinghua University
⁵University of Science and Technology of China ⁶The Chinese University of Hong Kong
^{*}Equal contribution [‡]Project lead [†]Corresponding author

Abstract

Closed-loop driving simulation requires real-time interaction beyond short offline clips, pushing current driving world models toward autoregressive (AR) rollout. Existing AR distillation approaches typically rely on frame sinks or student-side degradation training. The former transfers poorly to driving due to fast ego-motion and rapid scene changes, while the latter remains bounded by the teacher’s single-pass output length and thus provides only a limited supervision horizon. A natural question is: *can the teacher itself be extended via AR rollout to provide unbounded-horizon supervision at bounded memory cost?* The key difficulty is that a standard teacher drifts under its own predictions, contaminating the supervision it provides. Our key insight is to make the teacher rollout-capable, ensuring reliable supervision from its own AR rollouts. This is instantiated as HorizonDrive, an anti-drifting training-and-distillation framework for AR driving simulation. First, scheduled rollout recovery (SRR) trains the base model to reconstruct ground-truth future clips from prediction-corrupted histories, yielding a teacher that remains stable across long AR rollouts. Second, the rollout-capable teacher is extended via AR rollout, providing long-horizon distribution-matching supervision under bounded memory, while a short-window student aligns to it with teacher rollout DMD (TRD) for efficient real-time deployment. HorizonDrive natively supports minute-scale AR rollout under bounded memory; on nuScenes, HorizonDrive reduces FID by 52% and FVD by 37%, and lowers ARE and DTW by 21% and 9% relative to the strongest long-horizon streaming baselines, while remaining competitive with single-pass driving video generators. See project page at <https://zcliangyue.github.io/HorizonDrive>.

1 Introduction

Driving world models aim to serve as closed-loop simulation testbeds, where generated environments respond to an agent’s actions in real time. This requires long-horizon autoregressive (AR) rollout, in which the model repeatedly generates short future chunks, receives updated controls, and feeds its own predictions back as context. Such deployment induces exposure bias: each chunk is conditioned on imperfect generated frames rather than ground-truth observations, causing small errors to recursively compound into visual artifacts, geometric inconsistency, and semantic drift. As a result, even state-of-the-art driving world models (*e.g.*, Ren et al. [2025], Gao et al. [2025a]) degrade quickly, far short of the minute-scale horizons needed for meaningful closed-loop evaluation.

Recent work has begun to address this gap. Self-Forcing [Huang et al., 2025] trains an autoregressive student from a standard teacher diffusion model by conditioning each chunk on the student’s previous

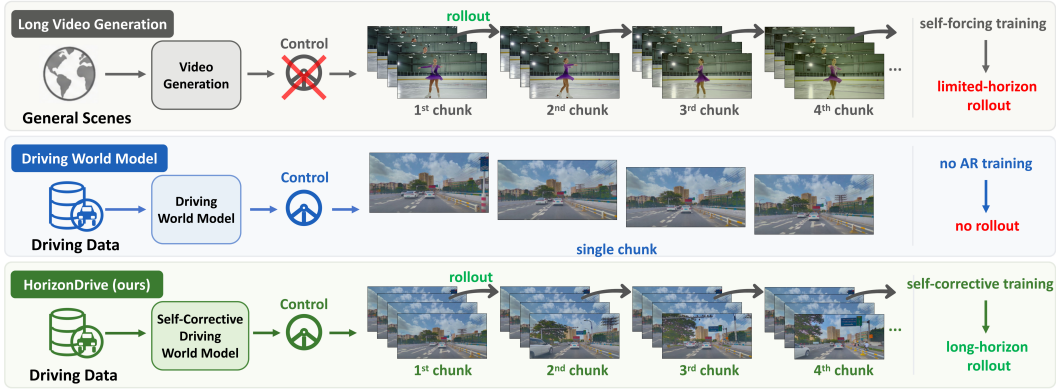


Figure 1: **Comparison with general long-video generators and driving world models.** General long-video generators can roll out but lack driving-specific control and suffer from drift, while existing driving world models cannot roll out autoregressively. HorizonDrive enables both action-controllable generation and stable long-horizon AR rollout, supporting real-time interactive driving simulation.

outputs rather than ground truth, exposing it to realistic rollout errors. While this improves rollout stability, the corrective signal is still limited to the teacher’s fixed single-pass generation window. Extending this window is impractical, as the attention cost of DiT grows quadratically with sequence length and quickly exceeds memory limits. Consequently, the supervision horizon remains capped by the teacher’s single-pass capacity, making long-horizon AR distillation hard to scale.

A natural question then arises: *can the teacher itself be extended to arbitrary horizons through AR rollout, providing unbounded supervision at constant memory cost?* We show that this is possible once the teacher is first made rollout-capable: by remaining stable under its own predicted context, the teacher breaks the single-pass horizon barrier and extends supervision through AR rollout. Based on this insight, we propose **HorizonDrive**, a two-stage anti-drifting distillation framework for real-time autoregressive driving simulation.

In the first stage, *Scheduled Rollout Recovery (SRR)*, we convert a standard driving world model into a rollout-capable teacher. This departs from conventional anti-drifting paradigms, which mainly regularize the deployed generator; instead, SRR stabilizes the supervisor so that long-horizon distillation is no longer confined to a clean, single-pass teacher window. SRR trains the teacher to recover clean future dynamics from prediction-corrupted histories, with a joint local-and-global schedule that smooths pred-to-GT transitions and shifts training from severe late-rollout drift to finer early-rollout correction. This enables stable repeated fixed-window rollout without relying on frame sinks or increasing single-pass memory cost.

In the second stage, we introduce *Teacher Rollout DMD (TRD)* to transfer long-horizon rollout behavior into a real-time student. The rollout-capable teacher provides stable long-horizon supervision through repeated fixed-window rollout, and TRD aligns the student to this teacher trajectory in a chunk-wise manner. This asymmetric design allows the teacher to generate longer chunks with more denoising steps, while the student generates shorter chunks with fewer steps for faster and finer-grained interaction. By rolling out multiple short student chunks to match the same teacher horizon, TRD enables an efficient student to inherit the teacher’s long-horizon stability.

Overall, HorizonDrive yields a short-chunk student that natively supports long-horizon AR rollout for interactive driving simulation. As summarized in Fig. 1, it bridges general long-video generation and driving world modeling by combining action-controllable generation with stable AR rollout. The student rolls out indefinitely with 10-frame chunks under bounded memory and can be extended to minute-scale horizons, while supporting multi-condition control (text, HD map, bounding boxes, and ego action). On nuScenes (where the per-clip length is bounded to ~ 20 s by the dataset), HorizonDrive reduces FID by 52% and FVD by 37%, and lowers ARE and DTW by 21% and 9% over the strongest long-horizon streaming baselines, while remaining competitive with single-pass driving video generators on short-clip evaluation; minute-scale rollout is further demonstrated qualitatively in the appendix.

Our contributions are threefold: (1) We identify rollout-capable teaching as the missing prerequisite for scalable long-horizon distillation and propose SRR to turn a standard driving world model into a

stable AR teacher. (2) We introduce TRD, which distills teacher rollout trajectories into a short-chunk, few-step student under bounded memory. (3) We provide a systematic evaluation on nuScenes, demonstrating that teacher-side rollout stabilization and chunk-wise rollout distillation substantially improve long-horizon visual quality and spatio-temporal consistency over strong streaming baselines.

2 Related Works

Conditional Video Generation for Autonomous Driving. Recent progress in video synthesis has been largely enabled by diffusion-based generative models [Peebles and Xie, 2023, Brooks et al., 2024, Gao et al., 2025b, RunwayML, 2024, Yang et al., 2024, Kong et al., 2024, Ma et al., 2025, Wan et al., 2025, Team et al., 2025]. Autonomous driving requires generation models to be both visually realistic and precisely controllable by structured scene conditions and driving behaviors. Existing methods often introduce geometric priors, including HD maps, 3D boxes, occupancy, and object-level spatial structures, to guide scene composition and agent placement [Wen et al., 2024, Wang et al., 2024b, Gao et al., 2024a, Zhao et al., 2025, Gao et al., 2025a]. Other methods use ego-motion or trajectory cues to control ego-vehicle behavior [Hu et al., 2023, Lu et al., 2024, Gao et al., 2024b, Zhang et al., 2025, Russell et al., 2025, Zhan et al., 2026]. Yet, most existing methods are limited by short generation horizons or high inference cost, restricting their use in closed-loop simulation.

Long Video Generation. Long-horizon video generation remains challenging, as models trained on short clips often accumulate temporal drift when extended to longer durations. Existing methods address this issue through training-free temporal extension, rollout-aware training, or inference-time stabilization. Qiu et al. [2023] and Kim et al. [2024] modify noise scheduling or reuse noisy contexts to extend short-video models. Chen et al. [2024] and Liu et al. [2025b] train with frame-wise independent noise to simulate corrupted histories, enabling autoregressive generation at inference time. Other efforts explore next-frame prediction with inverted sampling [Zhang and Agrawala, 2025], causal rollout training [Huang et al., 2025], error-bank mechanisms [Guo et al., 2025, Li et al., 2025], keyframe sinking [Huang et al., 2024a, Xiao et al., 2025, Zhou et al., 2024], test-time training [Dalal et al., 2025], and multi-shot generation [Cai et al., 2025]. Despite these advances, existing methods still suffer from drift beyond the training horizon.

Efficient Video Generation via Diffusion Distillation. Diffusion-based video models rely on iterative denoising, making inference cost a key obstacle to real-time generation. Recent methods accelerate sampling by distilling a multi-step teacher into a few-step student, using distribution matching [Yin et al., 2024b,a, Liu et al., 2025a, Wu et al., 2026] or consistency-style objectives [Song et al., 2023, Geng et al., 2024, 2025, Zheng et al., 2025]. Huang et al. [2025] further introduces rollout training to reduce the training-inference gap. However, distilled models can still accumulate errors during long-horizon autoregressive rollouts, limiting their robustness in closed-loop simulation. Our method performs teacher-rollout DMD, transferring long-horizon behavior from a stronger teacher to a short-chunk student while preserving efficient inference.

3 Preliminary

Diffusion models. In generative modeling, a diffusion process [Rombach et al., 2022, Esser et al., 2024, Blattmann et al., 2023, Brooks et al., 2024, Zheng et al., 2024] provides a continuous transformation of noise into structured data through a differential equation. This process models the evolution of latent variables, where each time step is controlled by a vector field v_Θ , defined as

$$dz_{(t)} = v_\Theta(z_{(t)}, t) dt, \quad t \in [0, 1]. \quad (1)$$

The latent variables $z_{(t)}$ evolve from random Gaussian noise ϵ at $t = 1$ to the data distribution at $t = 0$. The intermediate latent states are constructed as

$$z_{(t)} = \sigma_t z_{(0)} + (1 - \sigma_t) \epsilon, \quad (2)$$

where σ_t is a predefined noise schedule. The objective for recent flow matching formulation [Albergo and Vanden-Eijnden, 2022, Lipman et al., 2022, Liu et al., 2022] is defined by the v -prediction loss as

$$\mathcal{L}_{CFM} = \mathbb{E}_{\epsilon \sim \mathcal{N}(\mathbf{0}, \mathbf{I})} \|v_\Theta(z_{(t)}, t) - (z_{(0)} - \epsilon)\|_2^2. \quad (3)$$

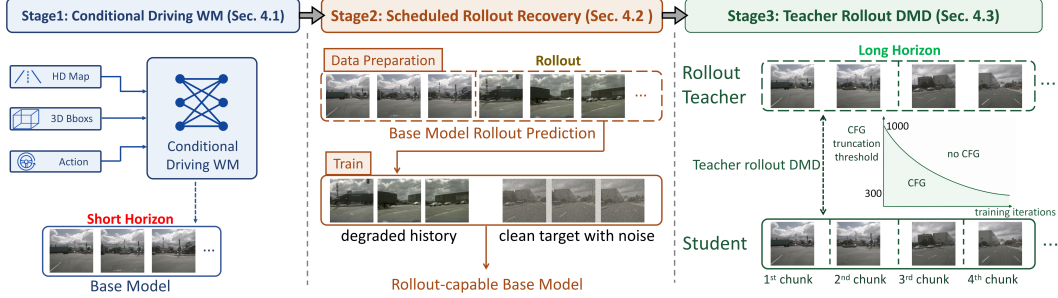


Figure 2: **Overview of HorizonDrive framework.** We first train a conditional driving world model, then improve its autoregressive stability through scheduled rollout recovery, and finally distill long-horizon teacher rollouts into a few-step, short-chunk student via teacher-rollout DMD.

Distribution matching distillation. Due to the slow inference speed of diffusion models, Distribution Matching Distillation (DMD) [Yin et al., 2024b] is applied to enhance real-time performance. DMD trains a few-step student model to match the teacher’s output distribution, thus reducing the inference overhead while maintaining high-quality generation. The loss gradient is defined as

$$\nabla_{\theta} \mathcal{L}_{DMD} = \mathbb{E}_{\tau} \left[- \left(s_{\text{real}}(z(\tau)) - s_{\text{fake}}(z(\tau)) \right) \right] \frac{\partial G_{\theta}}{\partial \theta}, \quad (4)$$

where τ is renosed level. This ensures similar generative quality between student and teacher models.

4 Methods

Problem formulation. We aim to build a real-time interactive autoregressive (AR) driving world model in a video-VAE latent space, where $\mathbf{z}_{1:T}$ denotes the AR context window and $\mathbf{c}_{T+1:T+K}$ denotes future driving controls over the next K frames. At each step, the model predicts the next K -frame chunk as

$$\hat{\mathbf{z}}_{T+1:T+K} \sim p_{\theta}(\mathbf{z}_{T+1:T+K} \mid \mathbf{z}_{1:T}, \mathbf{c}_{T+1:T+K}), \quad (5)$$

and appends it to the history buffer for the next step.

To realize this AR process, we instantiate HorizonDrive through three stages, as illustrated in Fig. 2. First, Sec. 4.1 trains a standard driving world model with robust multi-condition control, which serves as the foundation for subsequent autoregressive rollout. Second, Sec. 4.2 applies scheduled rollout recovery to convert this standard model into a rollout-capable teacher, enabling it to maintain stable generation under its own predicted histories. Finally, Sec. 4.3 performs teacher-rollout DMD, where the long-chunk, multi-step teacher provides rollout-consistent supervision for a short-chunk, few-step student.

4.1 Conditional driving world model training

The backbone of our conditional driving world model is a pretrained text-to-video (T2V) diffusion transformer with full bidirectional attention. To turn it into a video continuation model without modifying its architecture, we partition each training clip into a T -frame condition window and a K -frame generation chunk, and assign different noise levels to the two parts: condition latents $\mathbf{z}_{1:T}$ are kept clean with noise level $t=0$, while chunk latents $\mathbf{z}_{T+1:T+K}$ are noised and supervised with the flow-matching loss in Eq. (3).

To enable conditional control, we follow disentangled control [Ren et al., 2025, Russell et al., 2025, Zhan et al., 2026]: spatial scene structure (HD map, bounding boxes) is injected as additive layout tokens via a zero-initialized projector, while the residual ego-action signal $\mathbf{a}=(\Delta x, \Delta y, \Delta \text{yaw})$ is injected through AdaLN-style gating [Peebles and Xie, 2023]. Architectural details and the exact injection forms are deferred to Sec. A.

After training, we obtain a standard controllable driving world model, denoted as \mathcal{G}_0 . At inference, \mathcal{G}_0 rolls out long sequences via a sliding window: the most recent T latents form the next condition, a new K -frame chunk is generated via Eq. (5), and the context window is then shifted forward by K frames for the next AR step. However, since \mathcal{G}_0 is trained only with clean ground-truth histories, direct autoregressive rollout suffers from exposure bias.

4.2 SRR: scheduled rollout recovery training

To obtain a rollout-capable base model, instead of training on clean ground-truth clips, we sample segments from the rollout trajectory of \mathcal{G}_0 as degraded training conditions. Starting from a ground-truth latent history with length T , we roll out \mathcal{G}_0 for N autoregressive steps. At each step, the model predicts a chunk of K future latents and appends them to a fixed-length history buffer of size T :

$$\hat{\mathbf{z}}_{s_n+1:s_n+K} = \mathcal{G}_0(\hat{\mathbf{z}}_{s_n-T+1:s_n}, \mathbf{c}_{s_n+1:s_n+K}), \quad n = 1, \dots, N, \quad (6)$$

where $s_n = T + (n - 1)K$. This produces an N -step rollout trajectory $\hat{\mathbf{z}}_{T+1:T+NK}$, in which prediction errors accumulate across AR steps.

For a sampled starting index s for generation, we replace the conditioning history with rollout predictions while keeping the supervision target unchanged:

$$\tilde{\mathbf{z}}_{s-T+1:s} = \hat{\mathbf{z}}_{s-T+1:s}, \quad \mathbf{z}_{s+1:s+K}^* = \mathbf{z}_{s+1:s+K}. \quad (7)$$

As shown in Fig. 3 (a), we use two complementary schedules to make recovery training both smooth and progressive: a local pred-to-GT transition schedule within each sampled segment, and a global boundary-decay sampling schedule along the rollout trajectory.

Local pred-to-GT transition. Directly switching from the predicted history to the ground-truth future creates an abrupt temporal boundary. To smooth this transition, we introduce a pred-to-GT blending window of radius w around the generation boundary s . The final mixed training sequence $\bar{\mathbf{z}}_i$ is constructed as

$$\bar{\mathbf{z}}_i = \begin{cases} \tilde{\mathbf{z}}_i, & s - T + 1 \leq i \leq s - w, \\ \alpha_i \tilde{\mathbf{z}}_i + (1 - \alpha_i) \mathbf{z}_i^*, & s - w + 1 \leq i \leq s + w, \\ \mathbf{z}_i^*, & s + w + 1 \leq i \leq s + K, \end{cases} \quad (8)$$

where α_i linearly decreases from 1 to 0 within the transition window. This constructs a continuous temporal bridge from rollout-degraded latents to ground-truth latents around the boundary.

We further schedule the blending radius during training. At the beginning, we set $w = 0$, which exposes the model to a sharp boundary and encourages direct recovery from large rollout-induced deviations. As training progresses, w is gradually increased, expanding the transition region and shifting the task toward smoother, fine-grained correction.

Global boundary-decay sampling. We further schedule the sampled generation boundary s along the rollout trajectory. Here, the ranges 10–30, 30–50, 50–70, and 70–90 in Fig. 3 (b)(c) denote different boundary intervals of s from early to late rollout positions. The visualization reveals two complementary properties of rollout errors. First, the cross-case error heatmaps become progressively stronger as s moves toward later boundaries, indicating that longer autoregressive rollout leads to more severe accumulated degradation and semantic drift. Second, the off-diagonal cosine similarity is highest in the early boundary interval, showing that early-stage errors are more shared across cases, while later-stage semantic errors are more case-specific. Motivated by these observations, we adopt a boundary-decay curriculum: training starts from larger s , where the model is forced to recover from severe long-horizon semantic drift, and s is gradually decayed toward earlier rollout positions. This schedule first builds robustness to accumulated semantic failures and then refines the model on more generic, cross-case consistent rollout degradation.

Through scheduled rollout recovery (SRR), the initial conditional model \mathcal{G}_0 is transformed into a rollout-capable base model $\mathcal{G}_{\text{roll}}$, which learns to correct prediction-induced errors under realistic AR conditions and provides reliable long-horizon supervision for subsequent distillation.

4.3 TRD: teacher rollout DMD training

Despite its improved rollout stability, $\mathcal{G}_{\text{roll}}$ remains constrained by the high inference cost of multi-step diffusion sampling, making it impractical for real-time interactive simulation. We therefore distill it into a faster student through teacher rollout DMD training (TRD). Both the teacher $\mathcal{G}_{\text{roll}}^T$ and the student $\mathcal{G}_{\text{roll}}^S$ are initialized from $\mathcal{G}_{\text{roll}}$. The teacher is kept frozen, while only the student parameters ϕ are updated. They share the same conditioning window length T , but use different chunk sizes during generation. The teacher uses a longer chunk size K^T , while the student uses a shorter chunk size K^S , with $K^T > K^S$.

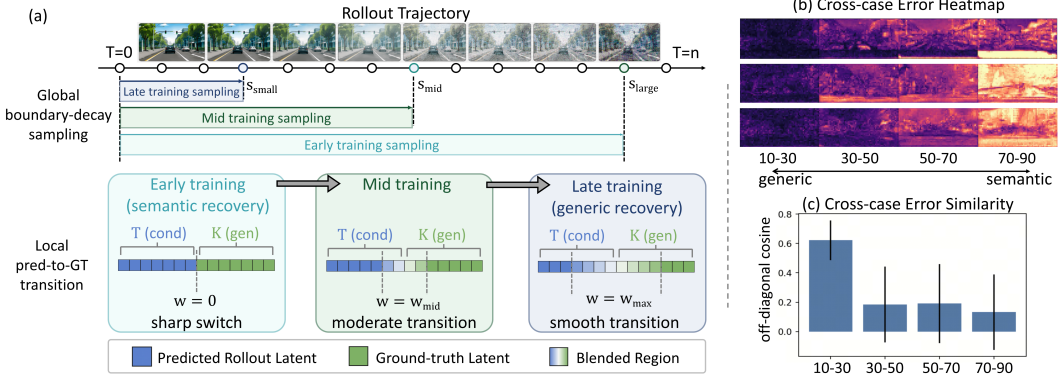


Figure 3: **Details of scheduled rollout recovery.** (a) Boundary-decay sampling gradually shifts training from late, semantically drifted rollout regions to earlier, more generic degradation, while pred-to-GT transition smooths the recovery target. (b) Error heatmaps reveal stronger semantic corruption at later rollout intervals. (c) Cross-case similarity shows that earlier errors are more consistent, supporting the proposed joint local-and-global schedule.

For long-horizon supervision beyond a single teacher chunk, we do not increase the teacher generation length. Instead, the teacher itself performs AR rollout with the fixed (T, K^T) window. This design keeps the teacher memory footprint fixed. The student also rolls out autoregressively with the fixed (T, K^S) window:

$$\hat{z}_{s_n+1:s_n+K^S}^S = \mathcal{G}_{\text{roll}, \phi}^S(\hat{z}_{s_n-T+1:s_n}^S, \mathbf{c}_{s_n+1:s_n+K^S}), \quad n = 1, \dots, N, \quad (9)$$

where ϕ denotes the student parameters. Whenever the accumulated student rollout covers a teacher-length interval K^T , we apply the DMD gradient to the latest K^T frames and immediately backpropagate. The frozen teacher rolls out over the same interval with its fixed (T, K^T) window to provide the distribution-matching direction. This step is repeated along the trajectory, transferring the teacher’s corrective ability to the student without accumulating memory across rollout steps.

Moreover, we adopt a noise-truncated CFG strategy. Standard DMD typically uses CFG to strengthen the teacher’s gradient guidance, but this tends to cause oversaturation during video rollout. Following Decoupled DMD [Liu et al., 2025a], we restrict CFG to noise levels below a threshold τ_{th} . We further schedule τ_{th} to decay during training, shifting the optimization focus from early conditional controllability to late-stage visual refinement.

Extending the standard DMD loss in (4), the TRD gradient is written as

$$\begin{aligned} \nabla_{\phi} \mathcal{L}_{\text{TRD}} = \mathbb{E}_{\tau} \left[- \left(\underbrace{s_{\text{cond}}^{\text{real}}(z(\tau)) - s_{\text{cond}}^{\text{fake}}(z(\tau))}_{\text{Distribution Matching}} \right. \right. \\ \left. \left. + \mathbf{1}_{\{\tau \leq \tau_{\text{th}}\}} (\alpha - 1) \underbrace{(s_{\text{cond}}^{\text{real}}(z(\tau)) - s_{\text{uncond}}^{\text{real}}(z(\tau)))}_{\text{Noise-truncated CFG}} \right) \frac{\partial \mathcal{G}_{\text{roll}, \phi}^S}{\partial \phi} \right], \quad (10) \end{aligned}$$

Overall, TRD uses a fixed-memory, long-chunk, multi-step teacher to supervise a short-chunk, few-step student along AR rollout trajectories. By aligning their chunk-wise distributions, the student inherits long-horizon generation behavior while substantially reducing per-chunk denoising latency and inference cost.

5 Experiments

5.1 Implementation

Implementation details. HorizonDrive is built on Wan 2.1 1.3B T2V [Wan et al., 2025] with the disentangled control modules of Sec. 4.1. For TRD, the teacher and student share a context window $T=11$, with chunk sizes $K^T=40$ (multi-step teacher) and $K^S=10$ (4-step student); the student rolls out $N=20$ AR steps during training. We use 700 nuScenes [Caesar et al., 2020] multi-view videos for training and 150 for validation; the per-clip length of ~ 20 s is the dataset upper bound and determines

our quantitative horizon, while longer minute-scale rollouts are shown qualitatively on a self-collected dataset (Sec. G). Full backbone, VAE, dataset, and optimization details are in Sec. A.

Evaluation metrics. We report **visual quality** via FID and FVD over the full rollout, as well as VBench [Huang et al., 2024b]. For **spatio-temporal consistency** (only applicable to methods with driving control), we recover per-frame poses with VGGT [Wang et al., 2025] and report **ARE** (mean geodesic rotation error vs. GT) and **DTW** (dynamic time warping distance between predicted and GT ego-motion trajectories [Keogh and Pazzani, 2000]); full definitions are in Sec. B.

5.2 Comparisons

Comparison methods. To ensure fair comparison across heterogeneous evaluation settings, we compare HorizonDrive against three groups of baselines on nuScenes; per-group evaluation protocols are detailed in Sec. C. (i) *Long-horizon interactive world model frameworks* (top group of Tab. 1) are end-to-end frameworks for long-horizon interactive world simulation, including Matrix-Game3 [Wang et al., 2026], Helios [Yuan et al., 2026], Causal-Forcing [Zhu et al., 2026], HY-WorldPlay [Sun et al., 2025], and LingBot-World [Team et al., 2026]; they do not natively accept our driving control signals, so we condition them only on the initial frames and report visual-quality metrics only. (ii) *Long-horizon streaming video generation methods* (bottom group of Tab. 1) are general anti-drifting recipes for streaming video generation, including Self-Forcing [Huang et al., 2025], Self-Forcing++ [Cui et al., 2025], and LongLive [Yang et al., 2025]; we re-train each under our base model and driving control modules so that architecture, base model, data, and conditioning are shared with HorizonDrive, isolating the long-horizon training framework as the only remaining variable. (iii) *Driving video generation models* (Tab. 2) are domain-specific generators (DriveDreamer [Wang et al., 2024a], Panacea [Wen et al., 2024], DreamForge [Mei et al., 2024], Vista [Gao et al., 2024b], MagicDrive-V2 [Gao et al., 2025a]) that accept driving control signals (actions, HD maps, bounding boxes) but generate only a fixed-length single-pass clip; most report metrics on short clips (8–25 frames), leaving long-video quality unexamined, so we evaluate in two groups—*short-video* and *long-video*—under each method’s original generation setting.

World model frameworks produce degraded visuals without driving control. The top group of Tab. 1 reports interactive world model frameworks that were not natively designed for driving and do not accept our control signals. Under our nuScenes long-rollout protocol, their visual fidelity is noticeably limited: FID ranges from 30.53 to 49.07 and FVD from 218.23 to 580.72, and their Image Quality scores (55.55–60.44) remain consistently below HorizonDrive’s 62.50. This highlights the importance of scene-specific driving control for faithful long-horizon driving simulation.

Self-correction outperforms naïve long-horizon streaming methods. The bottom group of Tab. 1 re-trains streaming anti-drifting methods on our base model and driving modules, ensuring identical architecture, data, and control signals—the only remaining variable is the long-horizon training framework itself. Even so, their visual quality remains consistently worse than HorizonDrive (FID 2–3× higher and FVD 1.6–1.7× higher), and their ego-motion consistency is also weaker on both ARE (3.28–3.78 vs. 2.60) and DTW (3.61–6.22 vs. 3.27), validating the effectiveness of our SRR–TRD framework. We attribute the gap to the fact that these baselines rely solely on long-horizon fine-tuning to mitigate drift, yet long tuning alone does not guarantee a rollout-capable teacher: a teacher that cannot reliably perform autoregressive rollout produces degraded trajectories, and distilling from poor supervision yields poor students. In contrast, SRR strengthens the teacher before distillation begins, raising the ceiling of what the student can learn. Error accumulation is more evident in Fig. 5, where the baseline’s FID degrades steadily with each autoregressive step while ours remains stable.

Driving-specific methods. Table 2 compares HorizonDrive with domain-specific driving generators. Since evaluation settings differ across methods, we report results from each method’s original paper for reference rather than as a strict ranking. In the short-video group, HorizonDrive with $N=1$ generates 21-frame clips that attain the best FVD (84.53) in the group, and its FID (12.54) is competitive with prior short-clip generators while uniquely supporting the full driving control suite (T+M+B+A) at the same chunk size used for long-video evaluation. In the long-video group, HorizonDrive rolls out $N=20$ steps autoregressively and matches MagicDrive-V2’s single-pass 241-frame quality (FVD 92.99 vs. 94.84, FID 13.82 vs. 20.91), suggesting that sequential rollout with few-step denoising can be competitive with many-step, single-pass generation. Together, these comparisons indicate that HorizonDrive delivers strong long-video quality for autonomous driving video generation.

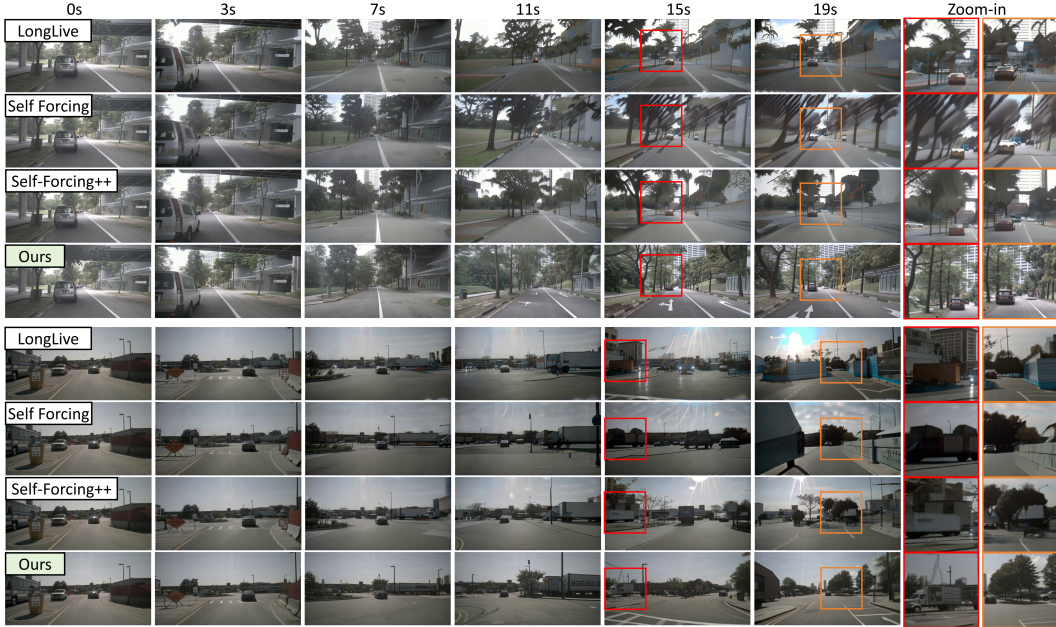


Figure 4: **Long-horizon rollout comparison with streaming video generation methods.** Our method preserves clearer scene structure, more stable object geometry, and better visual quality over time. See “zoom-in” for better details.

Table 1: **Comparison with long-horizon autoregressive video generation baselines on nuScenes val.** *Top group*: end-to-end interactive world model frameworks; they do not natively accept our driving control signals, so spatio-temporal consistency (ARE/DTW) is not applicable (“N/A”). *Bottom group*: general streaming video generation recipes re-trained on our base model and data with our driving control modules, where all metrics are reported. Best results are in **bold**.

Method	Visual		VBench			ST Cons.		
	FID↓	FVD↓	Qual.↑	Mot.↑	Img.↑	ARE↓	DTW↓	
<i>Long-horizon interactive world model frameworks</i>								
Matrix-Game3 [Wang et al., 2026]	35.69	338.22	78.99	93.78	60.44	N/A	N/A	
Helios [Yuan et al., 2026]	30.53	218.23	79.02	95.03	58.82	N/A	N/A	
Causal-Forcing [Zhu et al., 2026]	49.07	373.29	74.35	92.42	59.00	N/A	N/A	
HY-WorldPlay [Sun et al., 2025]	33.51	580.72	76.58	99.48	58.60	N/A	N/A	
LingBot-World [Team et al., 2026]	37.67	325.55	77.08	92.87	55.55	N/A	N/A	
<i>Long-horizon streaming video generation methods (re-trained on our base model and data)</i>								
Self-Forcing [Huang et al., 2025]	41.53	161.00	79.27	94.17	59.65	3.47	6.22	
Self-Forcing++ [Cui et al., 2025]	28.84	147.57	79.47	93.92	60.25	3.78	3.61	
LongLive [Yang et al., 2025]	29.05	161.41	79.35	93.46	60.80	3.28	3.65	
HorizonDrive (Ours)	13.82	92.99	79.53	93.85	62.50	2.60	3.27	

5.3 Ablation studies

We ablate three design choices in TRD: (1) whether the teacher and student are initialized from SRR-trained weights, (2) the number of autoregressive rollout steps N during training, and (3) the CFG augmentation strategy. The CFG threshold τ_{th} controls the maximum noise level at which CFG is applied in the DMD loss; we compare four schedules: **None** ($\tau_{th}=0$), **Full** ($\tau_{th}=1000$ throughout), **Early** (τ_{th} decays $1000 \rightarrow 0$ from step 0), and **Delayed** (τ_{th} decays $1000 \rightarrow 0$ after a 100-step warmup). Results are shown in Tab. 3.

Rollout-capable initialization benefits both teacher and student. When neither side is initialized from SRR (row 1, Base/Base), the model struggles with autoregressive error accumulation, producing the worst FVD (141.88) in this initialization group. Switching only the student to SRR (row 2, SRR/Base) yields a marginal gain on FVD and slightly worse FID (FID 19.24 \rightarrow 20.34, FVD

Table 2: **Comparison with driving video generation methods on nuScenes val.** Our distilled model achieves state-of-the-art FID and FVD both in the short-video and the long-video group.

Method	Unroll N	Frames	Conditions	FID ↓	FVD ↓
<i>Short-Video Evaluation</i>					
DriveDreamer [Wang et al., 2024a]	1	8	T+M+B	14.90	340.80
Panacea [Wen et al., 2024]	1	8	T+M+B	16.90	139.00
DreamForge [Mei et al., 2024]	1	16	T+M+B	14.61	103.61
Vista [Gao et al., 2024b]	1	25	T+A	6.90	89.40
HorizonDrive (Ours)	1	21	T+M+B+A	12.54	84.53
<i>Long-Video Evaluation</i>					
MagicDrive-V2 [Gao et al., 2025a]	1	241	T+M+B+A	20.91	94.84
HorizonDrive (Ours)	20	211	T+M+B+A	13.82	92.99

Conditions: T = text, M = HD map, B = bounding boxes, A = ego action.

Table 3: **Ablation of TRD design choices on nuScenes val.** Each group varies one factor while fixing the others. Init: student / teacher initialization (Base or SRR).

Init (Stu. / Tea.)	Unroll N	CFG	FID↓	FVD↓	ARE↓	DTW↓
Base / Base	20	Delayed	19.24	141.88	2.76	3.30
SRR / Base			20.34	128.77	3.15	3.39
Base / SRR			<u>14.44</u>	<u>107.54</u>	2.75	3.80
SRR / SRR	1	Delayed	21.15	135.35	3.39	5.42
	4		18.19	139.28	3.03	3.66
SRR / SRR	20	None	14.59	110.81	2.77	3.28
		Full	20.84	184.06	3.86	3.96
		Early	14.70	111.99	<u>2.64</u>	3.13
		Delayed	13.82	92.99	2.60	<u>3.27</u>

141.88→128.77): a rollout-aware student alone cannot compensate for a teacher that drifts under its own AR rollouts during TRD, and distilling from such degraded trajectories yields a degraded student. Switching only the teacher to SRR (row 3, Base/SRR) yields the largest single-factor gain (FID 19.24→14.44, FVD 141.88→107.54), confirming that *long-horizon supervision is dominated by the teacher’s rollout reliability*—a teacher that can reliably roll out provides high-quality trajectory targets even when the student starts from Base. Combining both (last row, SRR/SRR with our default $N=20$ and Delayed CFG) yields the best overall result (FID 13.82, FVD 92.99), showing that SRR is beneficial at both ends of the distillation pipeline while the teacher side carries the dominant effect.

Longer rollout during training improves long-horizon quality. With $N=1$, the student is only supervised on single-chunk generation and never experiences its own rollout errors, resulting in the worst ARE (3.39°) and DTW (5.42) in this group. As N grows, both ARE and DTW decrease monotonically (ARE: 3.39° → 3.03° → 2.60°; DTW: 5.42→3.66→3.27), and FVD drops sharply once N is large enough to expose the student to multi-step rollout errors (139.28 at $N=4$ → 92.99 at $N=20$). This confirms that longer autoregressive training chains are essential for deployment-time stability.

CFG augmentation benefits from noise-truncation. Directly applying CFG at all noise levels (Full) causes severe oversaturation, nearly doubling FVD to 184.06 compared to 110.81 without CFG. Early decay yields little improvement over no CFG, because DMD training itself requires few steps and the high-noise CFG is phased out before it can take effect. Delayed decay resolves this by allowing a warmup period for full-range CFG to establish strong conditional generation, then progressively restricting CFG to low noise levels to maintain visual quality, achieving the best FID (13.82), FVD (92.99), and ARE (2.60°); the Early schedule reaches a marginally better DTW (3.13 vs. 3.27) but at a sizeable cost in visual fidelity (FID 14.70 and FVD 111.99), and we therefore adopt Delayed decay as the default.

6 Conclusion and Limitations

We presented HorizonDrive, an anti-drifting distillation framework for long-horizon autonomous driving simulation. Instead of relying on frame sinks or student-side degradation alone, HorizonDrive first turns a standard video diffusion model into a rollout-capable teacher through scheduled rollout recovery, and then distills its long-horizon AR behavior into a short-chunk student with teacher rollout DMD. This design provides reliable long-horizon supervision under bounded memory and enables efficient AR deployment.

A key limitation is that SRR is conducted offline; future work will explore online rollout-recovery training, where the world model continuously improves its AR robustness from its own interaction trajectories.

References

- Michael S Albergo and Eric Vanden-Eijnden. Building normalizing flows with stochastic interpolants. *arXiv preprint arXiv:2209.15571*, 2022.
- Andreas Blattmann, Tim Dockhorn, Sumith Kulal, Daniel Mendelevitch, Maciej Kilian, Dominik Lorenz, Yam Levi, Zion English, Vikram Voleti, Adam Letts, et al. Stable video diffusion: Scaling latent video diffusion models to large datasets. *arXiv preprint arXiv:2311.15127*, 2023.
- Tim Brooks, Bill Peebles, Connor Holmes, Will DePue, Yufei Guo, Li Jing, David Schnurr, Joe Taylor, Troy Luhman, Eric Luhman, et al. Video generation models as world simulators. *OpenAI Blog*, 1(8):1, 2024.
- Holger Caesar, Varun Bankiti, Alex H Lang, Sourabh Vora, Venice Erin Liong, Qiang Xu, Anush Krishnan, Yu Pan, Giancarlo Baldan, and Oscar Beijbom. nuscenes: A multimodal dataset for autonomous driving. In *Proceedings of the IEEE/CVF conference on computer vision and pattern recognition*, pages 11621–11631, 2020.
- Shengqu Cai, Ceyuan Yang, Lvmin Zhang, Yuwei Guo, Junfei Xiao, Ziyang Yang, Yinghao Xu, Zhenheng Yang, Alan Yuille, Leonidas Guibas, et al. Mixture of contexts for long video generation. *arXiv preprint arXiv:2508.21058*, 2025.
- Boyuan Chen, Diego Martí Monsó, Yilun Du, Max Simchowitz, Russ Tedrake, and Vincent Sitzmann. Diffusion forcing: Next-token prediction meets full-sequence diffusion. *Advances in Neural Information Processing Systems*, 37:24081–24125, 2024.
- Justin Cui, Jie Wu, Ming Li, Tao Yang, Xiaojie Li, Rui Wang, Andrew Bai, Yuanhao Ban, and Cho-Jui Hsieh. Self-forcing++: Towards minute-scale high-quality video generation. *arXiv preprint arXiv:2510.02283*, 2025.
- Karan Dalal, Daniel Kocreja, Jiarui Xu, Yue Zhao, Shihao Han, Ka Chun Cheung, Jan Kautz, Yejin Choi, Yu Sun, and Xiaolong Wang. One-minute video generation with test-time training. In *Proceedings of the Computer Vision and Pattern Recognition Conference*, pages 17702–17711, 2025.
- Patrick Esser, Sumith Kulal, Andreas Blattmann, Rahim Entezari, Jonas Müller, Harry Saini, Yam Levi, Dominik Lorenz, Axel Sauer, Frederic Boesel, et al. Scaling rectified flow transformers for high-resolution image synthesis. In *Forty-first international conference on machine learning*, 2024.
- Ruiyuan Gao, Kai Chen, Zhihao Li, Lanqing Hong, Zhenguo Li, and Qiang Xu. Magicdrive3d: Controllable 3d generation for any-view rendering in street scenes. *arXiv preprint arXiv:2405.14475*, 2024a.
- Ruiyuan Gao, Kai Chen, Bo Xiao, Lanqing Hong, Zhenguo Li, and Qiang Xu. Magicdrive-v2: High-resolution long video generation for autonomous driving with adaptive control. In *Proceedings of the IEEE/CVF International Conference on Computer Vision*, pages 28135–28144, 2025a.
- Shenyuan Gao, Jiazhi Yang, Li Chen, Kashyap Chitta, Yihang Qiu, Andreas Geiger, Jun Zhang, and Hongyang Li. Vista: A generalizable driving world model with high fidelity and versatile controllability. *Advances in Neural Information Processing Systems*, 37:91560–91596, 2024b.
- Yu Gao, Haoyuan Guo, Tuyen Hoang, Weilin Huang, Lu Jiang, Fangyuan Kong, Huixia Li, Jiashi Li, Liang Li, Xiaojie Li, et al. Seedance 1.0: Exploring the boundaries of video generation models. *arXiv preprint arXiv:2506.09113*, 2025b.
- Zhengyang Geng, Ashwini Pokle, William Luo, Justin Lin, and J Zico Kolter. Consistency models made easy. *arXiv preprint arXiv:2406.14548*, 2024.

- Zhengyang Geng, Mingyang Deng, Xingjian Bai, J Zico Kolter, and Kaiming He. Mean flows for one-step generative modeling. *arXiv preprint arXiv:2505.13447*, 2025.
- Yuwei Guo, Ceyuan Yang, Hao He, Yang Zhao, Meng Wei, Zhenheng Yang, Weilin Huang, and Dahua Lin. End-to-end training for autoregressive video diffusion via self-resampling. *arXiv preprint arXiv:2512.15702*, 2025.
- Anthony Hu, Lloyd Russell, Hudson Yeo, Zak Murez, George Fedoseev, Alex Kendall, Jamie Shotton, and Gianluca Corrado. Gaia-1: A generative world model for autonomous driving. *arXiv preprint arXiv:2309.17080*, 2023.
- Lianghua Huang, Wei Wang, Zhi-Fan Wu, Yupeng Shi, Huanzhang Dou, Chen Liang, Yutong Feng, Yu Liu, and Jingren Zhou. In-context lora for diffusion transformers. *arXiv preprint arXiv:2410.23775*, 2024a.
- Xun Huang, Zhengqi Li, Guande He, Mingyuan Zhou, and Eli Shechtman. Self forcing: Bridging the train-test gap in autoregressive video diffusion. *arXiv preprint arXiv:2506.08009*, 2025.
- Ziqi Huang, Yanan He, Jiashuo Yu, Fan Zhang, Chenyang Si, Yuming Jiang, Yuanhan Zhang, Tianxing Wu, Qingyang Jin, Nattapol Chanpaisit, et al. Vbench: Comprehensive benchmark suite for video generative models. In *Proceedings of the IEEE/CVF Conference on Computer Vision and Pattern Recognition*, pages 21807–21818, 2024b.
- Eamonn J Keogh and Michael J Pazzani. Scaling up dynamic time warping for datamining applications. In *Proceedings of the sixth ACM SIGKDD international conference on Knowledge discovery and data mining*, pages 285–289, 2000.
- Jihwan Kim, Junoh Kang, Jinyoung Choi, and Bohyung Han. Fifo-diffusion: Generating infinite videos from text without training. *Advances in Neural Information Processing Systems*, 37:89834–89868, 2024.
- Wei jie Kong, Qi Tian, Zijian Zhang, Rox Min, Zuozhuo Dai, Jin Zhou, Jiangfeng Xiong, Xin Li, Bo Wu, Jianwei Zhang, et al. Hunyuanvideo: A systematic framework for large video generative models. *arXiv preprint arXiv:2412.03603*, 2024.
- Wuyang Li, Wentao Pan, Po-Chien Luan, Yang Gao, and Alexandre Alahi. Stable video infinity: Infinite-length video generation with error recycling. *arXiv preprint arXiv:2510.09212*, 2025.
- Yaron Lipman, Ricky TQ Chen, Heli Ben-Hamu, Maximilian Nickel, and Matt Le. Flow matching for generative modeling. *arXiv preprint arXiv:2210.02747*, 2022.
- Dongyang Liu, Peng Gao, David Liu, Ruoyi Du, Zhen Li, Qilong Wu, Xin Jin, Sihan Cao, Shifeng Zhang, Hongsheng Li, et al. Decoupled dmd: Cfg augmentation as the spear, distribution matching as the shield. *arXiv preprint arXiv:2511.22677*, 2025a.
- Kunhao Liu, Wenbo Hu, Jiale Xu, Ying Shan, and Shijian Lu. Rolling forcing: Autoregressive long video diffusion in real time. *arXiv preprint arXiv:2509.25161*, 2025b.
- Xingchao Liu, Chengyue Gong, and Qiang Liu. Flow straight and fast: Learning to generate and transfer data with rectified flow. *arXiv preprint arXiv:2209.03003*, 2022.
- Jiachen Lu, Ze Huang, Zeyu Yang, Jiahui Zhang, and Li Zhang. Wovogen: World volume-aware diffusion for controllable multi-camera driving scene generation. In *European Conference on Computer Vision*, pages 329–345. Springer, 2024.
- Guoqing Ma, Haoyang Huang, Kun Yan, Liangyu Chen, Nan Duan, Shengming Yin, Changyi Wan, Ranchen Ming, Xiaoniu Song, Xing Chen, et al. Step-video-t2v technical report: The practice, challenges, and future of video foundation model. *arXiv preprint arXiv:2502.10248*, 2025.
- Jianbiao Mei, Tao Hu, Xueming Yang, Licheng Wen, Yu Yang, Tiantian Wei, Yukai Ma, Min Dou, Botian Shi, and Yong Liu. Dreamforge: Motion-aware autoregressive video generation for multi-view driving scenes. *arXiv preprint arXiv:2409.04003*, 2024.
- William Peebles and Saining Xie. Scalable diffusion models with transformers. In *Proceedings of the IEEE/CVF international conference on computer vision*, pages 4195–4205, 2023.
- Haonan Qiu, Menghan Xia, Yong Zhang, Yingqing He, Xintao Wang, Ying Shan, and Ziwei Liu. Freenoise: Tuning-free longer video diffusion via noise rescheduling. *arXiv preprint arXiv:2310.15169*, 2023.

- Xuanchi Ren, Yifan Lu, Tianshi Cao, Ruiyuan Gao, Shengyu Huang, Amirmojtaba Sabour, Tianchang Shen, Tobias Pfaff, Jay Zhangjie Wu, Runjian Chen, Seung Wook Kim, Jun Gao, Laura Leal-Taixe, Mike Chen, Sanja Fidler, and Huan Ling. Cosmos-drive-dreams: Scalable synthetic driving data generation with world foundation models, 2025. URL <https://arxiv.org/abs/2506.09042>.
- Robin Rombach, Andreas Blattmann, Dominik Lorenz, Patrick Esser, and Björn Ommer. High-resolution image synthesis with latent diffusion models. In *Proceedings of the IEEE/CVF conference on computer vision and pattern recognition*, pages 10684–10695, 2022.
- GA RunwayML. Introducing gen-3 alpha: a new frontier for video generation, 2024.
- Lloyd Russell, Anthony Hu, Lorenzo Bertoni, George Fedoseev, Jamie Shotton, Elahe Arani, and Gianluca Corrado. Gaia-2: A controllable multi-view generative world model for autonomous driving. *arXiv preprint arXiv:2503.20523*, 2025.
- Yang Song, Prafulla Dhariwal, Mark Chen, and Ilya Sutskever. Consistency models. 2023.
- Wenqiang Sun, Haiyu Zhang, Haoyuan Wang, Junta Wu, Zehan Wang, Zhenwei Wang, Yunhong Wang, Jun Zhang, Tengfei Wang, and Chunchao Guo. Worldplay: Towards long-term geometric consistency for real-time interactive world modeling. *arXiv preprint arXiv:2512.14614*, 2025.
- Meituan LongCat Team, Xunliang Cai, Qilong Huang, Zhuoliang Kang, Hongyu Li, Shijun Liang, Liya Ma, Siyu Ren, Xiaoming Wei, Rixu Xie, et al. Longcat-video technical report. *arXiv preprint arXiv:2510.22200*, 2025.
- Robbyant Team, Zelin Gao, Qiuyu Wang, Yanhong Zeng, Jiapeng Zhu, Ka Leong Cheng, Yixuan Li, Hanlin Wang, Yinghao Xu, Shuailei Ma, et al. Advancing open-source world models. *arXiv preprint arXiv:2601.20540*, 2026.
- Team Wan, Ang Wang, Baole Ai, Bin Wen, Chaojie Mao, Chen-Wei Xie, Di Chen, Fei Wu Yu, Haiming Zhao, Jianxiao Yang, et al. Wan: Open and advanced large-scale video generative models. *arXiv preprint arXiv:2503.20314*, 2025.
- Jianyuan Wang, Minghao Chen, Nikita Karaev, Andrea Vedaldi, Christian Rupprecht, and David Novotny. Vggt: Visual geometry grounded transformer. In *Proceedings of the Computer Vision and Pattern Recognition Conference*, pages 5294–5306, 2025.
- Xiaofeng Wang, Zheng Zhu, Guan Huang, Xinze Chen, Jiagang Zhu, and Jiwen Lu. Drivedreamer: Towards real-world-drive world models for autonomous driving. In *European conference on computer vision*, pages 55–72. Springer, 2024a.
- Yuqi Wang, Jiawei He, Lue Fan, Hongxin Li, Yuntao Chen, and Zhaoxiang Zhang. Driving into the future: Multiview visual forecasting and planning with world model for autonomous driving. In *Proceedings of the IEEE/CVF Conference on Computer Vision and Pattern Recognition*, pages 14749–14759, 2024b.
- Zile Wang, Zexiang Liu, Jaixing Li, Kaichen Huang, Baixin Xu, Fei Kang, Mengyin An, Peiyu Wang, Biao Jiang, Yichen Wei, et al. Matrix-game 3.0: Real-time and streaming interactive world model with long-horizon memory. *arXiv preprint arXiv:2604.08995*, 2026.
- Yuqing Wen, Yucheng Zhao, Yingfei Liu, Fan Jia, Yanhui Wang, Chong Luo, Chi Zhang, Tiancai Wang, Xiaoyan Sun, and Xiangyu Zhang. Panacea: Panoramic and controllable video generation for autonomous driving. In *Proceedings of the IEEE/CVF Conference on Computer Vision and Pattern Recognition*, pages 6902–6912, 2024.
- Tianhe Wu, Ruibin Li, Lei Zhang, and Kede Ma. Diversity-preserved distribution matching distillation for fast visual synthesis. *arXiv preprint arXiv:2602.03139*, 2026.
- Junfei Xiao, Ceyuan Yang, Lvmin Zhang, Shengqu Cai, Yang Zhao, Yuwei Guo, Gordon Wetzstein, Maneesh Agrawala, Alan Yuille, and Lu Jiang. Captain cinema: Towards short movie generation. In *The Fourteenth International Conference on Learning Representations*, 2025.
- Shuai Yang, Wei Huang, Ruihang Chu, Yicheng Xiao, Yuyang Zhao, Xianbang Wang, Muyang Li, Enze Xie, Yingcong Chen, Yao Lu, et al. Longlive: Real-time interactive long video generation. *arXiv preprint arXiv:2509.22622*, 2025.
- Zhuoyi Yang, Jiayan Teng, Wendi Zheng, Ming Ding, Shiyu Huang, Jiazheng Xu, Yuanming Yang, Wenyi Hong, Xiaohan Zhang, Guanyu Feng, et al. Cogvideox: Text-to-video diffusion models with an expert transformer. *arXiv preprint arXiv:2408.06072*, 2024.

- Tianwei Yin, Michaël Gharbi, Taesung Park, Richard Zhang, Eli Shechtman, Fredo Durand, and William T Freeman. Improved distribution matching distillation for fast image synthesis. *Advances in neural information processing systems*, 37:47455–47487, 2024a.
- Tianwei Yin, Michaël Gharbi, Richard Zhang, Eli Shechtman, Fredo Durand, William T Freeman, and Taesung Park. One-step diffusion with distribution matching distillation. In *Proceedings of the IEEE/CVF conference on computer vision and pattern recognition*, pages 6613–6623, 2024b.
- Shenghai Yuan, Yuanyang Yin, Zongjian Li, Xinwei Huang, Xiao Yang, and Li Yuan. Helios: Real real-time long video generation model. *arXiv preprint arXiv:2603.04379*, 2026.
- Yifan Zhan, Zhengqing Chen, Qingjie Wang, Zhuo He, Muyao Niu, Xiaoyang Guo, Wei Yin, Weiqiang Ren, Qian Zhang, and Yinqiang Zheng. Composing driving worlds through disentangled control for adversarial scenario generation. *arXiv preprint arXiv:2603.12864*, 2026.
- Kaiwen Zhang, Zhenyu Tang, Xiaotao Hu, Xingang Pan, Xiaoyang Guo, Yuan Liu, Jingwei Huang, Li Yuan, Qian Zhang, Xiao-Xiao Long, et al. Epona: Autoregressive diffusion world model for autonomous driving. *arXiv preprint arXiv:2506.24113*, 2025.
- Lvmin Zhang and Maneesh Agrawala. Packing input frame context in next-frame prediction models for video generation. *arXiv e-prints*, pages arXiv–2504, 2025.
- Guosheng Zhao, Xiaofeng Wang, Zheng Zhu, Xinze Chen, Guan Huang, Xiaoyi Bao, and Xingang Wang. Drivedreamer-2: Llm-enhanced world models for diverse driving video generation. In *Proceedings of the AAAI Conference on Artificial Intelligence*, volume 39, pages 10412–10420, 2025.
- Kaiwen Zheng, Yuji Wang, Qianli Ma, Huayu Chen, Jintao Zhang, Yogesh Balaji, Jianfei Chen, Ming-Yu Liu, Jun Zhu, and Qinsheng Zhang. Large scale diffusion distillation via score-regularized continuous-time consistency. *arXiv preprint arXiv:2510.08431*, 2025.
- Zangwei Zheng, Xiangyu Peng, Tianji Yang, Chenhui Shen, Shenggui Li, Hongxin Liu, Yukun Zhou, Tianyi Li, and Yang You. Open-sora: Democratizing efficient video production for all, 2024. URL <https://github.com/hpcaitech/Open-Sora>, 2024.
- Yupeng Zhou, Daquan Zhou, Ming-Ming Cheng, Jiashi Feng, and Qibin Hou. Storydiffusion: Consistent self-attention for long-range image and video generation. *Advances in Neural Information Processing Systems*, 37:110315–110340, 2024.
- Hongzhou Zhu, Min Zhao, Guande He, Hang Su, Chongxuan Li, and Jun Zhu. Causal forcing: Autoregressive diffusion distillation done right for high-quality real-time interactive video generation. *arXiv preprint arXiv:2602.02214*, 2026.

A Implementation details

Backbone and VAE. HorizonDrive is built on Wan 2.1 1.3B [Wan et al., 2025] with full bidirectional attention, and adopts the disentangled driving-control modules described in Sec. 4.1. Since driving scenes involve fast ego-motion and rapidly changing fine details, we fine-tune the original VAE to reduce its temporal compression ratio from 4 to 1, preserving full temporal resolution for higher visual fidelity.

Conditional control modules. We elaborate on the disentangled control architecture summarized in Sec. 4.1. HD map and bounding box information are first rendered as structural conditions $z_{b_f} \in \mathbb{R}^{c \times f \times h \times w}$, processed by a lightweight convolutional adapter, and reshaped into layout tokens $h_{b_f} \in \mathbb{R}^{f \times s \times d}$. The evolving feature representation at diffusion time t , denoted $h_{(t)}$, is updated by adding the projected layout tokens following $h_{(t)} \leftarrow h_{(t)} + f_{\text{zero}}(h_{b_f})$, where $f_{\text{zero}}(\cdot)$ is a zero-initialized projector. Action control is injected by computing the relative transformation $\Delta \mathbf{T}_i = \mathbf{T}_i^{-1} \mathbf{T}_{i+1}$ from a continuous trajectory of shape $F \times 4 \times 4$. We extract the residual signal $\mathbf{a} = (\Delta x, \Delta y, \Delta \text{yaw}) \in \mathbb{R}^{F \times 3}$ and inject it via AdaLN-style gating [Peebles and Xie, 2023] as $f_{\text{zero}}(\phi(\mathbf{a})) \in \mathbb{R}^{f \times 6 \times d}$, where $\phi(\cdot)$ is the sinusoidal frequency embedding. The resulting six channels are split into two groups, representing the pre-normalization shift/scale and post-layer residual gate for self-attention and feed-forward sublayers, respectively.

Training stages. We first train the base conditional driving world model \mathcal{G}_0 for 40K steps on a 100-hour proprietary driving dataset and 10K steps on nuScenes [Caesar et al., 2020], using short clips of length $T+K$ with ground-truth conditioning latents. We then apply SRR for 10K steps on nuScenes to obtain $\mathcal{G}_{\text{roll}}$; SRR keeps the same (T, K) but maintains a per-clip rollout cache refreshed every R optimizer steps with the current θ , uses a decaying AR rollout depth $N(k)$, samples the boundary index s in $[T, T+N(k)K]$ within each clip, and gradually enlarges the blending radius w . For TRD distillation, the SRR-initialized teacher and student share a context window of $T=11$ frames; the teacher generates $K^T=40$ frames per chunk and slides a $(T+K^T)=51$ -frame supervision window across its rollout to cover each student chunk, providing memory-bounded supervision over the long-horizon trajectory, while the student generates $K^S=10$ new frames per chunk with $M^S=4$ denoising steps and rolls out $N=20$ autoregressive steps. TRD updates the chunk-wise distribution matching loss every D student chunks; CFG augmentation is applied only at low noise levels ($\tau \leq \tau_{\text{th}}$) with weight α . Full optimization hyperparameters and stage-specific schedules are listed in Tabs. 4 and 5.

Datasets and evaluation horizon. For nuScenes [Caesar et al., 2020], we use 700 multi-view videos of ~ 20 seconds for training and 150 for validation; the per-clip length of ~ 20 s is the dataset upper bound, which determines the horizon of our quantitative evaluation. Longer rollouts of up to one minute on a self-collected dataset are demonstrated qualitatively in Sec. G.

Inference efficiency. With our temporally-uncompressed VAE and a 4-step student denoiser, each AR rollout step generates one $K^S=10$ -frame chunk on a single NVIDIA 5090 GPU. The per-chunk wall-clock latency is **1.8 s** at 256×512 resolution and **5.8 s** at 384×768 , yielding effective generation rates of ~ 5.6 FPS and ~ 1.7 FPS, respectively. Because the rolling-window rollout (Sec. 4.1) bounds per-step compute by $T+K^S$ regardless of total horizon, this per-chunk latency is sustained throughout the rollout, enabling stable streaming generation up to minute-scale horizons (Sec. G).

B Evaluation metrics

Visual quality. We report Fréchet Inception Distance (FID) and Fréchet Video Distance (FVD) computed over the full rollout sequence, as well as VBench [Huang et al., 2024b] as an overall video-quality measure.

Spatio-temporal consistency. These metrics are applicable only to methods that accept driving control signals. We recover per-frame camera poses from both generated and ground-truth videos with VGGT [Wang et al., 2025]. **ARE** (Average Rotation Error) measures the mean geodesic distance between predicted and GT rotation matrices across frames, reflecting heading accuracy. **DTW** (Dynamic Time Warping) [Keogh and Pazzani, 2000] aligns predicted and GT ego-motion trajectories via non-rigid time warping and computes the cumulative Euclidean distance under the optimal alignment, capturing path-shape fidelity even under temporal misalignment.

Table 4: **Training configuration of the teacher stages of HorizonDrive.** “–” marks entries not applicable to the corresponding stage.

Hyperparameter	Base (\mathcal{G}_0)	SRR ($\mathcal{G}_{\text{roll}}$)
Optimizer	AdamW	AdamW
Learning rate	1e-5	1e-5
Weight decay	1e-2	1e-5
Global batch size	96	64
Mixed precision	bf16	bf16
Training steps	40K (proprietary) + 10K (nuScenes)	10K (nuScenes)
GPU Usage	96 NVIDIA 5090	64 NVIDIA 5090
Context window length T	11	11
Chunk size K	10, 40	10, 40
Resolution	[256, 512], [384, 768]	[256, 512], [384, 768]
AR rollout depth N	–	$N(k)$ schedule
Cache refresh period R (optimizer steps)	–	2000
$N(k)$ schedule (start \rightarrow end)	–	10 \rightarrow 4 (steps 0-8000)
Blending radius w schedule	–	0 \rightarrow 8 (steps 0-8000)

Table 5: **Training configuration of the distillation stage (TRD).**

Hyperparameter	TRD
Optimizer	AdamW
Student learning rate	2e-6
Critic learning rate	1e-5
Weight decay	0.1
Batch size	32
Mixed precision	bf16
Training steps	200
GPU Usage	32 NVIDIA 5090
Context window length T	11
Chunk size K	10 (student) / 40 (teacher)
AR rollout depth N	20 (student)
Denoising steps	4
DMD update interval D (student chunks)	5
CFG threshold τ_{th} schedule	1000 (steps 0–100), decay \rightarrow 0 (step 400)
CFG scale α	6

C Baseline evaluation protocols

Group (i): long-horizon interactive world model frameworks. These methods are designed for general open-domain or interactive world simulation and do not natively accept our driving control signals (actions, HD maps, bounding boxes). For each method, we use the publicly released checkpoint, condition it only on the initial frame(s) following the original interface, and let it autoregressively roll out to match our nuScenes evaluation horizon. We report visual-quality metrics (FID, FVD, VBench) only; ego-motion consistency (ARE/DTW) is marked “N/A” since no driving control is provided.

Group (ii): long-horizon streaming video generation methods. Self-Forcing [Huang et al., 2025], Self-Forcing++ [Cui et al., 2025], and LongLive [Yang et al., 2025] are general streaming long-video recipes. To ensure fair comparison, for each baseline we (a) attach our disentangled driving control modules (Sec. 4.1) to the same Wan 2.1 1.3B backbone, (b) initialize from our base model \mathcal{G}_0 , and (c) re-train using each method’s original training recipe (loss, scheduler, rollout configuration, hyperparameters) on our nuScenes training split. Architecture, base model, training data, and driving conditioning are therefore shared with HorizonDrive, so the only remaining variable is the long-horizon training framework itself. All metrics (FID, FVD, VBench, ARE, DTW) are reported under the same protocol as HorizonDrive.

Group (iii): driving video generation models. These are domain-specific driving generators that accept driving control signals but produce only a fixed-length single-pass clip (8–241 frames depending on the method). Since each method’s evaluation setting differs (clip length, validation split, conditioning, evaluation protocol), we directly take FID/FVD numbers from the original papers

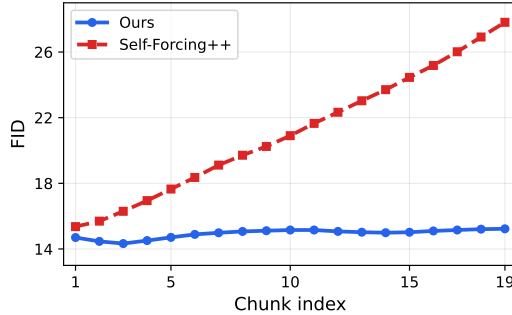


Figure 5: Long-horizon generation quality comparison.

and report them in two groups—*short-video* (8–25 frames) and *long-video* (241 frames)—rather than re-running them under a unified protocol. Results in this table are intended as a domain reference rather than a strict head-to-head ranking.

D Error accumulation analysis

Fig. 5 reports the FID computed on each cumulative chunk during autoregressive rollout. Our method maintains stable image quality across all 19 chunks, with no accumulation of error over the rollout horizon. In contrast, Self-Forcing++ suffers from compounding errors that cause FID to degrade monotonically, confirming that our self-rollout recovery training yields significantly stronger robustness to the distribution shift encountered during long-horizon autoregressive generation.

E Additional qualitative results on nuScenes

We provide additional rollouts on nuScenes val to complement the quantitative comparison in the main paper. Figures 6 to 8 compare HorizonDrive against the long-horizon streaming baselines (Self-Forcing, Self-Forcing++, LongLive) under our shared base model and driving control conditions. Figures 9 and 10 compare against representative driving world models that are not autoregressive (e.g., Matrix-Game3, Helios, LingBot-World), where each method uses its own native generation setting. Across both groups, HorizonDrive preserves road structure, agent layout, and spatio-temporal consistency throughout the rollout, while baselines progressively drift in geometry, color, or scene composition.

F Results on the self-collected dataset

To evaluate generalization beyond nuScenes, we also benchmark on our internal self-collected end-to-end (e2e) driving dataset, which features higher ego speeds and more diverse scenarios than nuScenes. Table 6 reports the quantitative comparison against the long-horizon streaming baselines under the same protocol as the main paper (re-trained on our base model and the e2e training split, evaluated on a held-out split). Figures 11 and 12 provide qualitative rollouts. HorizonDrive again outperforms all baselines on visual quality (FID/FVD), VBench dimensions, and spatio-temporal consistency, indicating that the rollout-capable base model and TRD distillation transfer to a substantially different driving distribution.

G Minute-level autoregressive generation

HorizonDrive supports minute-level AR generation under bounded per-step memory and compute, which is otherwise infeasible for single-pass video diffusion baselines whose memory grows quadratically with sequence length. At inference, the sliding-window rollout (Sec. 4.1) keeps each step’s compute bounded by $T+K^S$, so the model can be rolled out indefinitely without re-warming the cache. Figure 13 shows a continuous rollout of approximately one minute on the self-collected dataset (10 FPS, $K^S=10$, $T=11$), where the model maintains coherent road geometry, lane structure, and traffic-agent behavior throughout the rollout, demonstrating practical viability for closed-loop driving simulation.

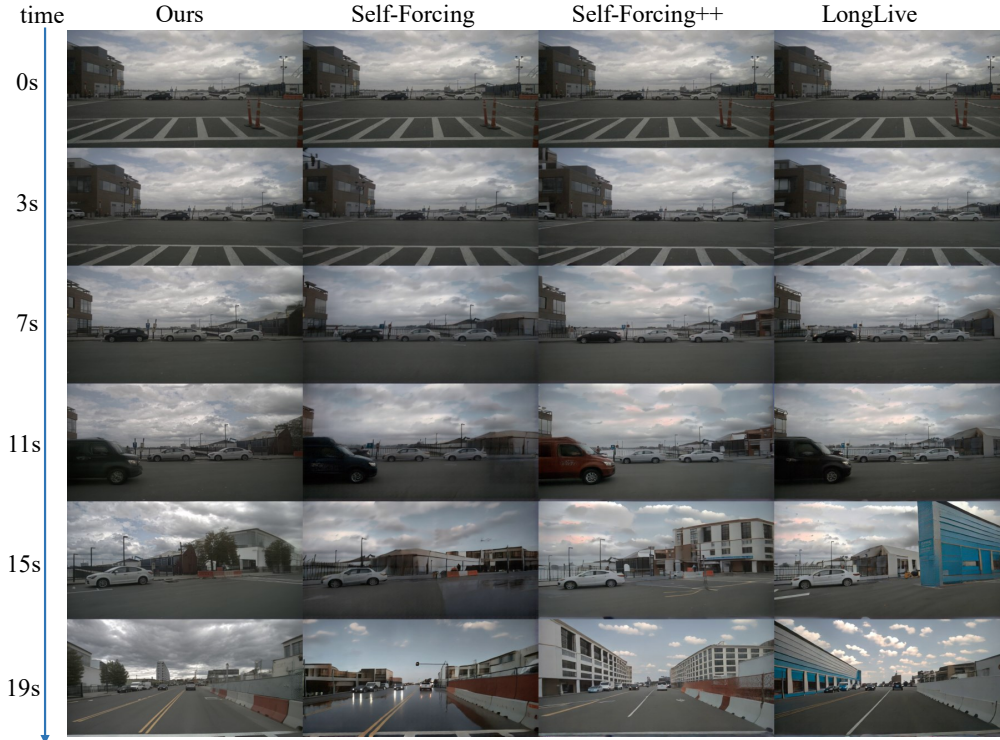


Figure 6: **Qualitative comparison with long-horizon streaming baselines on nuScenes val (scene 1).** From left to right: HorizonDrive, Self-Forcing, Self-Forcing++, LongLive

Table 6: **Comparison with long-horizon streaming video generation baselines on the self-collected (e2e) dataset.** All baselines share our base model and driving control modules, and are re-trained on the e2e training split following each method’s original recipe. Best results are in **bold**; second best are underlined.

Method	Visual		VBench			ST Cons.	
	FID↓	FVD↓	Qual.↑	Mot.↑	Img.↑	ARE↓	DTW↓
<i>Long-horizon streaming video generation methods (re-trained on our base model and e2e data)</i>							
Self-Forcing [Huang et al., 2025]	58.23	561.11	76.68	94.48	<u>63.18</u>	5.43	14.13
Self-Forcing++ [Cui et al., 2025]	66.93	534.36	74.54	92.70	59.12	7.32	18.40
LongLive [Yang et al., 2025]	<u>28.39</u>	<u>374.94</u>	<u>78.18</u>	<u>94.57</u>	62.53	<u>4.05</u>	<u>8.11</u>
HorizonDrive (Ours)	12.01	117.27	80.12	95.22	67.65	3.67	5.29

H Closed-loop driving simulation

We further evaluate HorizonDrive in a closed-loop driving simulation setup, where a planner and the world model interact step by step: at each AR step, the planner consumes the latest generated frame and outputs an ego trajectory, which is re-encoded (together with the corresponding HD map and bounding-box layouts) as the next-step action condition fed back into HorizonDrive, and the loop repeats indefinitely under the same bounded per-step memory budget as standard rollout (Sec. G). No ground-truth ego trajectory is used during simulation, so every conditioning signal beyond the initial frame is self-generated. As shown in Fig. 14, despite the compounding of rollout error from the world model and prediction error from the planner, HorizonDrive maintains coherent road geometry, lane topology, and stable agent behavior throughout the rollout, demonstrating practical viability for closed-loop policy evaluation under self-generated ego trajectories.

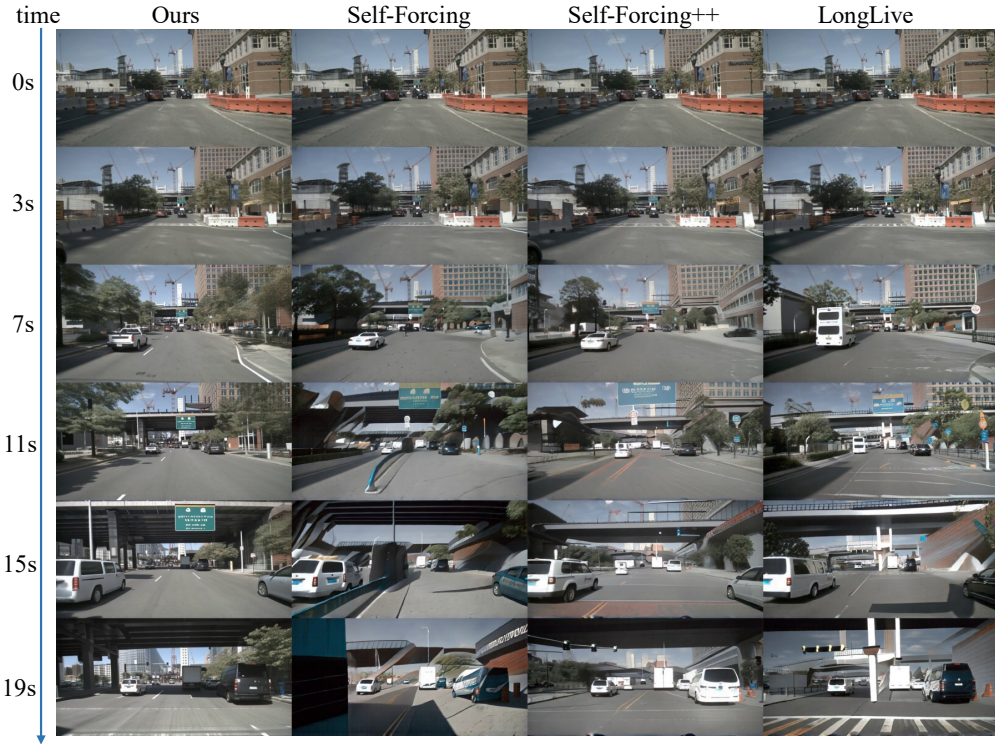


Figure 7: **Qualitative comparison with long-horizon streaming baselines on nuScenes val (scene 2).**

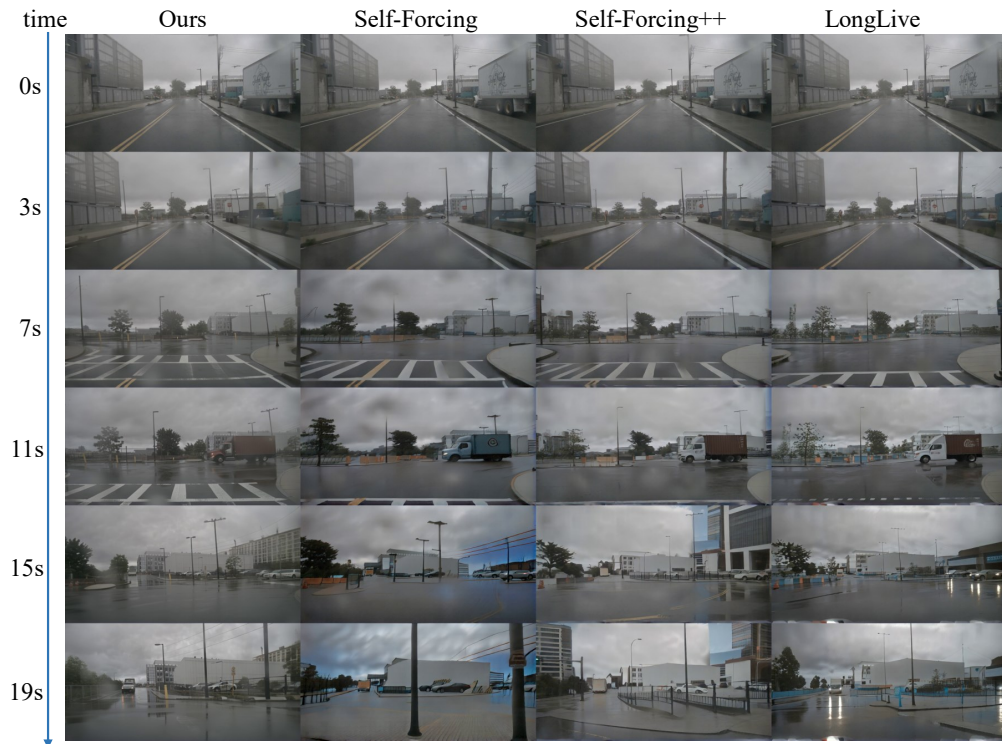


Figure 8: **Qualitative comparison with long-horizon streaming baselines on nuScenes val (scene 3).** Same layout as Fig. 6.

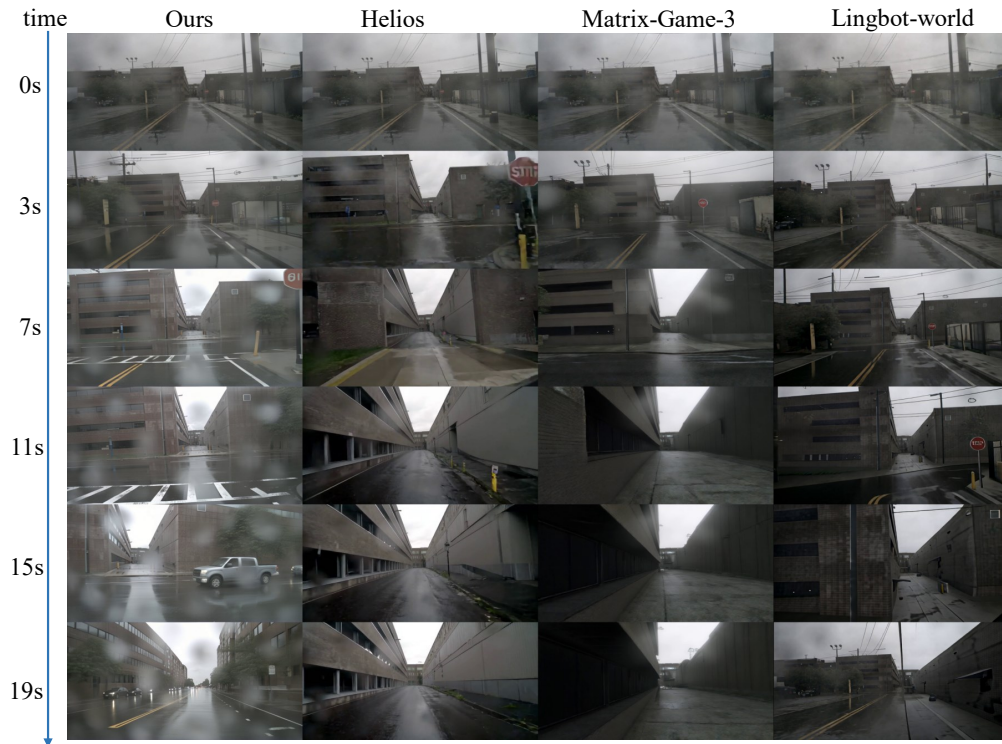


Figure 9: **Qualitative comparison with driving world models on nuScenes val (scene 1).** From left to right: HorizonDrive, Helios, Matrix-Game3, LingBot-World



Figure 10: **Qualitative comparison with driving world models on nuScenes val (scene 2).**



Figure 11: **Qualitative comparison with long-horizon streaming baselines on the self-collected (e2e) dataset (scene 1).** From left to right: HorizonDrive, Self-Forcing, Self-Forcing++, LongLive

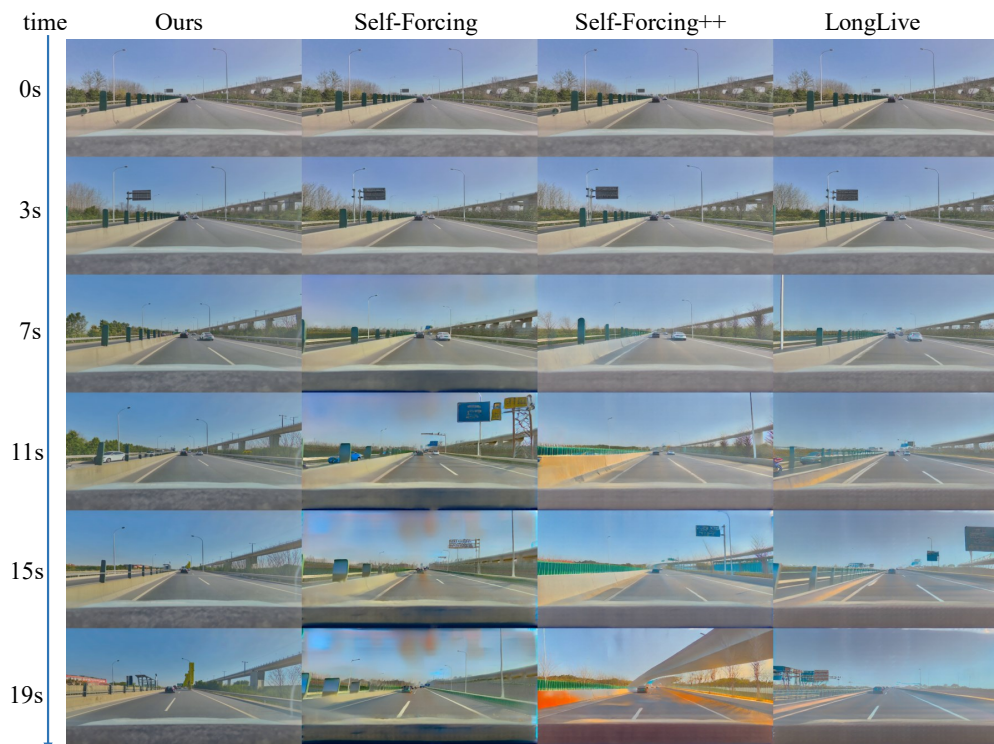


Figure 12: **Qualitative rollouts on the self-collected (e2e) dataset (scene 2).**

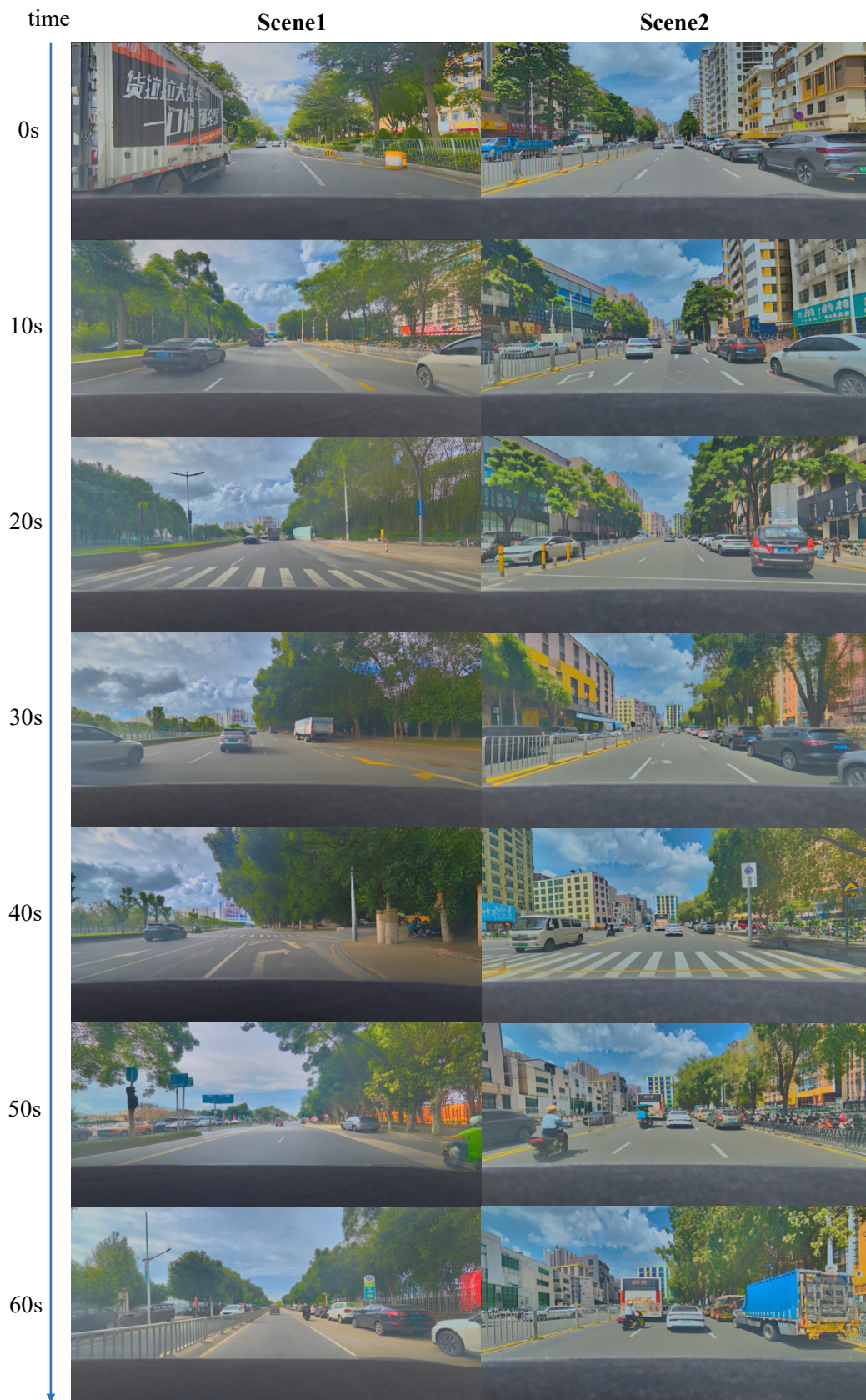


Figure 13: Minute-level autoregressive generation on the self-collected (e2e) dataset.

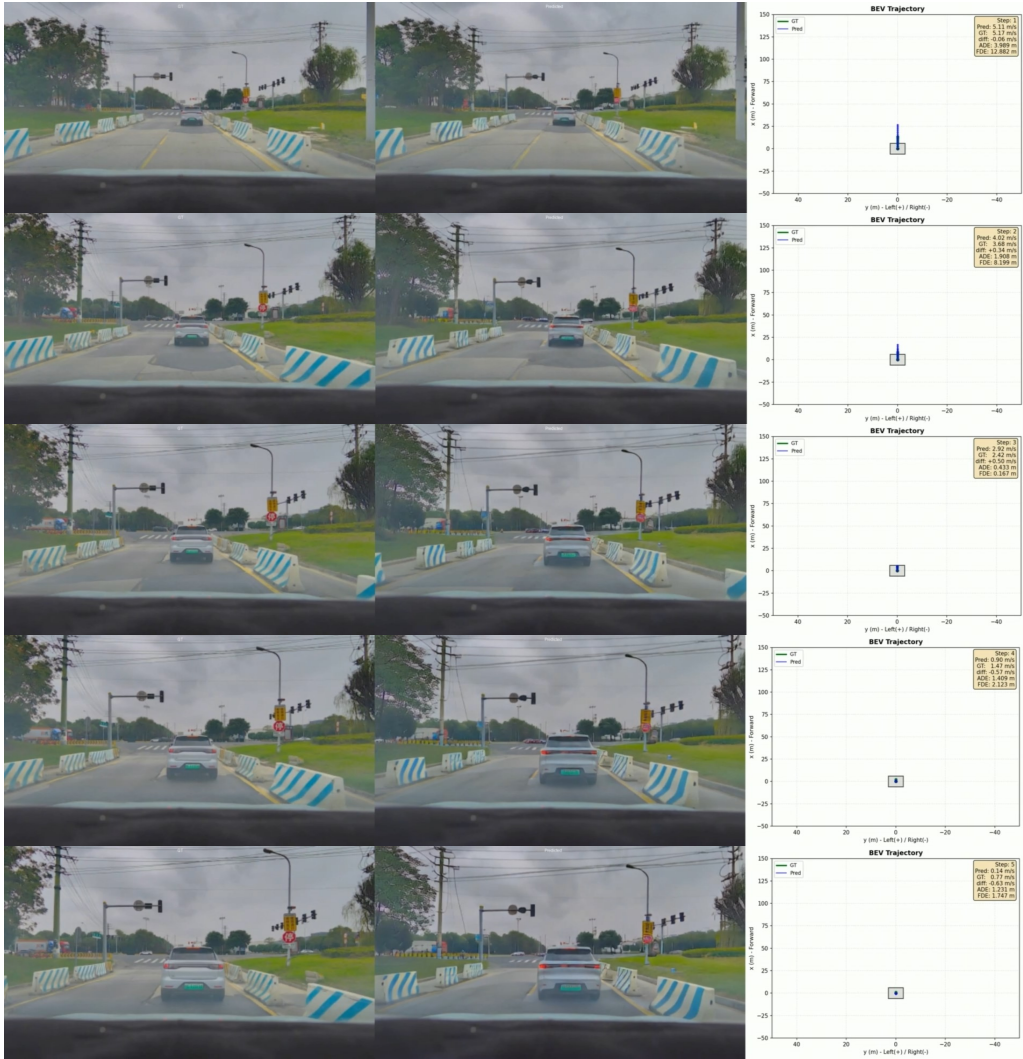


Figure 14: **Closed-loop driving simulation.** A planner consumes the latest generated frame at each step and outputs an ego trajectory, which HorizonDrive uses as the next-step action condition. Despite the planner-and-world-model loop being driven entirely by self-generated signals, HorizonDrive maintains coherent scene structure and stable agent behavior over long horizons.